

Photo-Transmutation of Leptons

José BORDES

jose.m.bordes@uv.es

*Departament Fisica Teorica, Universitat de Valencia,
calle Dr. Moliner 50, E-46100 Burjassot (Valencia), Spain*

CHAN Hong-Mo

chanhm@v2.rl.ac.uk

*Rutherford Appleton Laboratory,
Chilton, Didcot, Oxon, OX11 0QX, United Kingdom*

Jacqueline FARIDANI

jfarida@osfi-bsif.gc.ca

*Office of the Superintendent of Financial Institutions of Canada,
121 King St. W., Toronto, ON M5H 3T9, Canada*

TSOU Sheung Tsun

tsou@maths.ox.ac.uk

*Mathematical Institute, University of Oxford,
24-29 St. Giles', Oxford, OX1 3LB, United Kingdom*

Abstract

By photo-transmutation of leptons we mean photon-lepton reactions of the following type: $\gamma l_\alpha \rightarrow \gamma l_\beta$ with $l_\alpha \neq l_\beta$, occurring as a consequence of the lepton mass matrix changing its orientation (rotating) under changing scales. In this paper, we first discuss these reactions in general terms, then proceed to the calculation of their cross sections in two specific schemes, one within the framework of the conventional Standard Model, the other being the so-called Dualized Standard Model we ourselves advocate. Although the cross section obtained is generally small the calculation reveals certain special circumstances where these reactions may be accessible to experiment, for example with virtual photons in LEP for $\gamma e \rightarrow \gamma \tau$, and in BEPC for $\gamma e \rightarrow \gamma \mu$.

1 Introduction

By photo-transmutation of leptons, we mean the class of reactions:

$$\gamma + l_\alpha \longrightarrow \gamma + l_\beta, \quad (1.1)$$

with l_α and l_β being two different charged lepton states, which can occur in consequence of the lepton mass matrix changing its orientation in generations space (rotates) with changing energy scales [1]. Such reactions, of course, do not occur when the lepton states e , μ , or τ are, and remain, eigenstates of the lepton mass matrix. But if the mass matrix rotates with changing scales, as is seen to be the case [2] in the Standard Model when there is nontrivial mixing between up- and down-states [3, 4], then at any scale other than that at which the leptons states are defined as eigenstates, the mass matrix will no longer be diagonal and transmutational reactions such as (1.1) with $\alpha \neq \beta$ can occur. This is a special case of a general class of fermion transmutation phenomena arising from rotating fermion mass matrices, for a more detailed discussion of which the reader is referred to our companion paper [2].

Given that in recent experiments on neutrino oscillations [5, 6, 7], appreciable lepton mixing is indicated, it is already incumbent upon us, even when working within the present Standard Model framework, to investigate whether transmutational effects can be observed, although these are generally expected to be small. Going beyond the Standard Model, however, especially in schemes aimed at explaining the generation puzzle such as the Dualized Standard Model that we ourselves advocate [8, 9, 10, 11, 12], such an investigation becomes imperative, since there may then be other forces driving the rotation of the fermion mass matrix, leading to enhancements of transmutational effects beyond that given above by nontrivial mixing in the Standard Model. It would thus be important to check for the consistency of such schemes whether the transmutational effects they predict would remain within the present experimental bounds and, if they do, whether they may be accessible to experimental tests in the not too distant future.

The photo-transmutation of leptons (1.1) is one of the simplest example we could find of transmutational effects to calculate, and also probably one of the most easily accessible to experimental scrutiny. We propose therefore to examine this in some detail below both for general interest and with the ulterior motive of testing our Dualized Standard Model.

To leading order in perturbation theory, the cross section for the process (1.1) is given by the Feynman diagrams in Figure 1 which are formally the same as those for ordinary Compton scattering except that the lepton mass

matrix pertaining to the lepton lines in the diagrams, referring as it does to the energy scale \sqrt{s} at which the experiment is performed, would in general be nondiagonal in the physical lepton states e, μ , and τ as identified in the incoming and outgoing lepton beams. Because of this peculiarity, some care is needed in adapting the usual Feynman rules to this case.

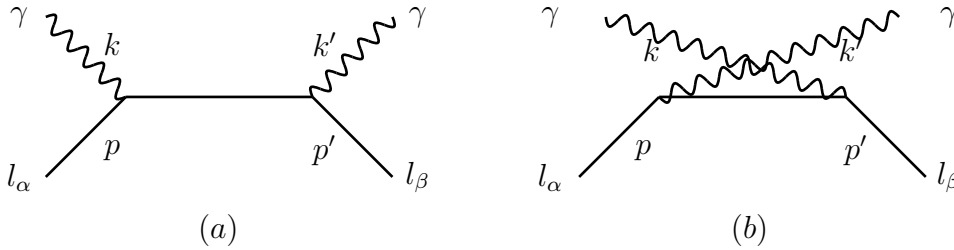


Figure 1: Compton-like diagrams for photo-transmutation of leptons

2 Kinematics

To measure the cross section of a transmutation process, say e.g. $\gamma\mu \rightarrow \gamma e$, one would send in a beam of muons and install downstream a detector for electrons. However, in the case that the lepton mass matrix rotates, as we have discussed in some detail in our companion paper [2], both what we call a muon and what we call an electron have to be defined at some prescribed scales. Two prescriptions were considered, for details of which the reader is referred to that paper: (i) “fixed scale diagonalization” (FSD) where the state vectors for the leptons of all 3 generations are defined at the same chosen scale, and (ii) “step-by-step diagonalization” (SSD) where the state vectors for the 3 leptons are each defined at its own mass scale. The two prescriptions differ in that the mass matrix is diagonal in (i) only at the chosen scale but in (ii) whenever the scale equals any of the 3 lepton masses. In either case, however, since the mass matrix rotates, the state vectors thus defined have no reason to be eigenstates of the mass matrix at the scale of the scattering energy \sqrt{s} at which the transmutation measurement is carried out. This means that from the point of view of the experiment, neither the incoming muon nor the outgoing electron has a definite mass. Instead, each will be a linear combination of the states with definite masses at the scale

of the scattering energy, namely the eigenstates of the mass matrix at that scale with the eigenvalues m_i .

At the scattering scale, therefore, let us write the state vector of an “external” (i.e. incoming or outgoing) state U_α as:

$$U_\alpha = S_{\alpha i} U_i, \quad (2.1)$$

where

$$U_1 = \begin{pmatrix} u_1 \\ 0 \\ 0 \end{pmatrix}; \quad U_2 = \begin{pmatrix} 0 \\ u_2 \\ 0 \end{pmatrix}; \quad U_3 = \begin{pmatrix} 0 \\ 0 \\ u_3 \end{pmatrix}, \quad (2.2)$$

with $S_{\alpha i}$ being the rotation matrix relating the external state α to the “internal states” i . Each u_i , being a state with a definite mass m_i at the scale under consideration, can be assigned a definite 4-momentum p_i satisfying the mass condition $p_i^2 = m_i^2$ and be taken as a solution of the free Dirac equation:

$$(\not{p}_i - m_i)u_i(p_i) = 0. \quad (2.3)$$

The state U_α at the same scale, however, does not have a definite mass, and therefore cannot be assigned a definite 4-momentum, although, of course, it has a mass m_α and a 4-momentum p at the scale where it is defined as an eigenstate. In trying to evaluate the Feynman diagrams (a) and (b) of Figure 1, the question then arises how the momenta p_i of the eigenstates $u_i(p_i)$ should be related first, to one another, and secondly, to the incoming (outgoing) momentum p (p') of the lepton states l_α (l_β).

To answer this question, we recall a more familiar but parallel situation in neutrino oscillations. A muon neutrino ν_μ there, not being an eigenstate of the mass matrix, has also no definite 4-momentum, but can be expressed as a linear combination of the mass eigenstates $\nu_i, i = 1, 2, 3$, each of which can be assigned a definite 4-momentum p_i . As to how these p_i are related to one another and to the given momentum of the ν_μ beam, the answer depends on the problem being investigated. In the case that the incoming ν_μ beam is given a definite 3-momentum \mathbf{p} say, then the 3-momenta \mathbf{p}_i by definition are all equal to \mathbf{p} , but the energies $E_i = \sqrt{\mathbf{p}_i^2 + m_i^2}$ have to differ, and one has neutrino oscillations in time as the beam propagates. On the other hand, in the case that the incoming ν_μ is given a definite energy, E say, which is more likely in most experimental situations, then the energies E_i are all equal to E , but the 3-momenta \mathbf{p}_i differ, and one has neutrino oscillations in distance (i.e. the baseline). Hence, by analogy one sees that the answer to the question asked in the last paragraph will also depend on the problem

addressed. Since we have already specified that the diagrams (a) and (b) of Figure 1 are to be evaluated at the scale \sqrt{s} , we have already ascribed to these diagrams a definite s , namely that:

$$s = (p + k)^2 = (p_i + k)^2, \quad (2.4)$$

common both to the incoming (outgoing) channels α (β) and to all eigenchannels i , which means that in this case, in contrast to the above example in neutrino oscillations, neither the 3-momentum nor the energy, but only s will have a definite value.

To evaluate the Feynman diagrams, we shall need the explicit relations between the different momenta p_i . Given 4-momentum conservation:

$$p_i + k = p'_i + k', \quad (2.5)$$

we note first that the 4-momentum transfer

$$t = (k - k')^2 = (p_i - p'_i)^2 \quad (2.6)$$

is also the same for all i , since k and k' , being the photon momenta, have nothing to do with the rotation of the fermion states. Expressing then p_j as a linear combination of k, k' and p_i :

$$p_j = a_j k + b_j k' + c_j p_i. \quad (2.7)$$

and imposing the conditions (2.4) and:

$$p_i^2 = p'_i{}^2 = m_i^2, \quad (2.8)$$

we obtain:

$$\begin{aligned} c_j &= \sqrt{\frac{(s - m_j^2)^2 + st}{(s - m_i^2)^2 + st}}, \\ b_j &= \frac{c_j(s - m_i^2) - (s - m_j^2)}{t}, \\ a_j &= \frac{c_j(s + t - m_i^2) - (s + t - m_j^2)}{t}. \end{aligned} \quad (2.9)$$

Similarly, expressing p'_j as:

$$p'_j = a'_j k' + b'_j k + c'_j p_i, \quad (2.10)$$

we obtain:

$$c'_j = c_j; \quad b'_j = b_j; \quad a'_j = a_j. \quad (2.11)$$

It is easy to check that the above relations between p_i 's and p'_i 's are both reflexive and transitive as they should be and that, in spite of appearance, are nonsingular at $t = 0$.

Equivalently, the relations between the momenta derived in the preceding paragraph may be expressed in terms of scalar products as follows:

$$(p_i k) = \frac{1}{2}(s - m_i^2), \quad (2.12)$$

$$(p_i k') = \frac{1}{2}(s + t - m_i^2), \quad (2.13)$$

$$(p_i p_j) = \frac{1}{t} \sqrt{[(s - m_i^2)(s + t - m_i^2) + m_i^2 t][(s - m_j^2)(s + t - m_j^2) + m_j^2 t]} \\ - \frac{1}{2t} [(s - m_i^2)(s + t - m_j^2) + (s - m_j^2)(s + t - m_i^2)], \quad (2.14)$$

$$(p_i p'_j) = \frac{1}{t} \sqrt{[(s - m_i^2)(s + t - m_i^2) + m_i^2 t][(s - m_j^2)(s + t - m_j^2) + m_j^2 t]} \\ - \frac{1}{2t} [(s + t - m_i^2)(s + t - m_j^2) + (s - m_j^2)(s - m_i^2)], \quad (2.15)$$

together with some similar relations for p'_i , which may be convenient for invariant calculations in the future.

However, for reasons which will be made clear later, we shall in this paper be working in a specific Lorentz frame, namely the cm frame of one chosen channel, say i , i.e. in the frame where the 3-momenta:

$$\mathbf{p}_i + \mathbf{k} = \mathbf{p}'_i + \mathbf{k}' = 0. \quad (2.16)$$

This does not correspond in general to the cm frame for another internal channel, say j , given the way that the internal momenta p_i and p_j are related. Labelling in the chosen i cm frame the angles and 3-momenta for the various particles as in Figure 2, we can write their momenta as:

$$\begin{aligned} k &= (\omega_i, 0, 0, \omega_i), \\ k' &= (\omega_i, 0, \omega_i \sin \theta'_i, \omega_i \cos \theta'_i), \\ p_i &= (E_i, 0, 0, -\omega_i), \\ p'_i &= (E_i, 0, -\omega_i \sin \theta'_i, -\omega_i \cos \theta'_i), \\ p_j &= (E_j, 0, -\omega_j \sin \theta_j, -\omega_j \cos \theta_j), \\ p'_j &= (E_j, 0, -\omega_j \sin \theta'_j, -\omega_j \cos \theta'_j), \end{aligned} \quad (2.17)$$

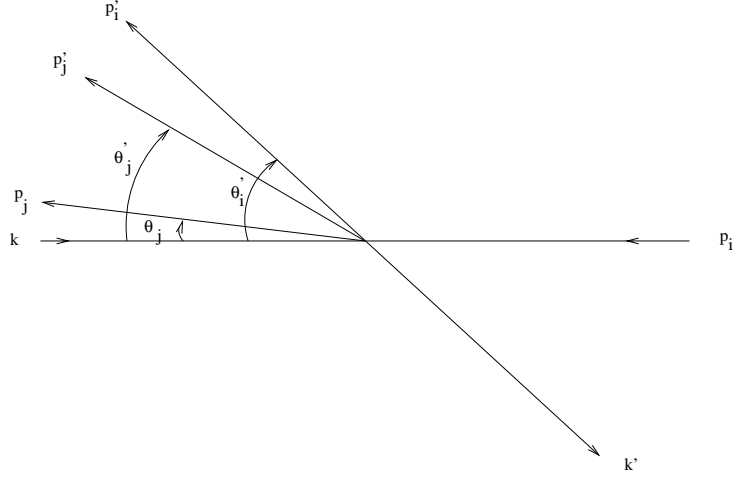


Figure 2: The 3-momenta of the various particles in the i cm frame

with

$$E_i = \frac{s + m_i^2}{2\sqrt{s}}, \quad (2.18)$$

$$\omega_i = \frac{s - m_i^2}{2\sqrt{s}}, \quad (2.19)$$

$$\cos \theta'_i = 1 + \frac{2st}{(s - m_i^2)^2}. \quad (2.20)$$

Hence, from (2.7), (2.10), (2.9), and (2.11), one easily obtains in terms of the invariants s and t :

$$E_j = \frac{1}{2\sqrt{st}} [2\sqrt{\{(s - m_j^2)^2 + st\}\{(s - m_i^2)^2 + st\}} - (s - m_i^2)\{2(s - m_j^2) + t\}], \quad (2.21)$$

with

$$\omega_j = \sqrt{E_j^2 - m_j^2}, \quad (2.22)$$

and

$$\sin \theta_j = \frac{1}{\sqrt{s}} \frac{1}{\sqrt{-t}} \frac{1}{2\omega_i \omega_j} [(s - m_i^2)\sqrt{(s - m_j^2)^2 + st} - (s - m_j^2)\sqrt{(s - m_i^2)^2 + st}], \quad (2.23)$$

$$\sin \theta'_j = \frac{1}{\sqrt{s}} \frac{1}{\sqrt{-t}} \frac{1}{2\omega_i \omega_j} [(s - m_i^2)\sqrt{(s - m_j^2)^2 + st} - (s - m_j^2 + t)\sqrt{(s - m_i^2)^2 + st}], \quad (2.24)$$

with

$$\theta'_i = \theta_j + \theta'_j. \quad (2.25)$$

Again, in spite of appearance, these formulae are all nonsingular at $t = 0$. They will be useful later for the calculation of the cross section.

3 The Invariant Amplitude

The amplitude to leading order for the transmutation process (1.1) is then by (2.1) given as:

$$\mathcal{M} = \sum_i S_{\beta i}^* \mathcal{M}_i S_{\alpha i}, \quad (3.1)$$

where we have made use of the fact that the lepton mass matrix, and hence also the scattering matrix, is diagonal in the (internal) states i . Each \mathcal{M}_i is a sum of two terms corresponding respectively to the two diagrams (a) and (b) of Figure 1:

$$\mathcal{M}_i = \mathcal{M}_i^{(a)} + \mathcal{M}_i^{(b)}, \quad (3.2)$$

with

$$\mathcal{M}_i^{(a)} = -ie^2 \bar{u}(p'_i) \not{\epsilon}^*(k') \frac{(\not{p}_i + \not{k}') + m_i}{(p_i + k)^2 - m_i^2} \not{\epsilon}(k) u(p_i), \quad (3.3)$$

and

$$\mathcal{M}_i^{(b)} = -ie^2 \bar{u}(p'_i) \not{\epsilon}(k) \frac{(\not{p}_i - \not{k}') + m_i}{(p_i - k')^2 - m_i^2} \not{\epsilon}^*(k') u_i(p_i). \quad (3.4)$$

Notice that although the last two formulae are formally the same as in ordinary Compton scattering, the quantities m_i and p_i which enter are both dependent on the energy scale \sqrt{s} .

Given the rotation $S_{\alpha i}$ and the unusual kinematics both of which depend rather intricately on the energy scale, a check on some basic properties of the amplitude is warranted. First, we wish to be assured that the amplitude (3.1) vanishes at all scales if we put either $\epsilon(k) \rightarrow k$ or $\epsilon(k') \rightarrow k'$ as required by gauge invariance. This is indeed true for on putting $\epsilon(k) = k$ and using the equation of motion (2.3), one obtains for the contribution of the s -channel diagram (a) to \mathcal{M} as:

$$\mathcal{M}^{(a)} \longrightarrow -ie^2 \sum_i S_{\beta i}^* \bar{u}(p'_i) \not{\epsilon}(k') u(p_i) S_{\alpha i}, \quad (3.5)$$

but for the contribution of the u -channel diagram (b) as:

$$\mathcal{M}^{(b)} \longrightarrow ie^2 \sum_i S_{\beta i}^* \bar{u}(p'_i) \not{\epsilon}(k') u(p_i) S_{\alpha i}, \quad (3.6)$$

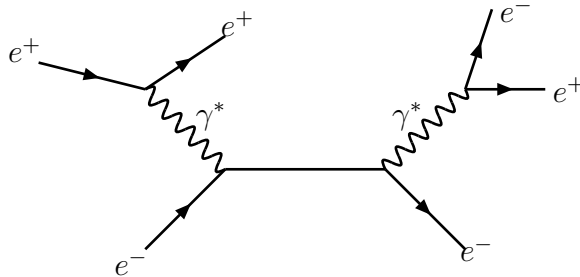


Figure 3: Feynman diagram for the reaction $e^+e^- \rightarrow e^+e^-e^+e^-$

so that the two terms do indeed cancel as required at any scale. A similar conclusion obtains also when we put $\epsilon(k') \rightarrow k'$.

Next, we wish to check that the amplitude \mathcal{M} has sensible pole structures. Consider first the s -channel poles which according to (3.3) can occur at $(p_i + k)^2 = m_i^2$, or equivalently by (2.4) at $s = m_i^2$, when the denominator vanishes. For the actual reaction $\gamma l_i \rightarrow \gamma l_i$ with real photons, however, $s = m_i^2$ corresponds to the reaction threshold where the numerator in the amplitude also vanishes so that the pole is cancelled, corresponding to the fact that the Compton cross section is finite in the Thomson limit. But if the photon is taken off mass-shell, then the cancellation need not work and a pole can occur. Consider first the simpler situation at energies below the τ mass where the mass matrix is only 2-dimensional, with the higher of its two eigenvalues, m_2 say, coinciding by definition with m_μ as $\sqrt{s} \rightarrow \mu$. The amplitude $\gamma^* l_2 \rightarrow \gamma^* l_2$ will thus develop a pole at $s = m_\mu^2$, but the amplitude for the other internal channel $\gamma^* l_3 \rightarrow \gamma^* l_3$, of course, will not have this pole. Consider now, however, the amplitudes for the processes $\gamma^* \mu \rightarrow \gamma^* \mu$ and $\gamma^* e \rightarrow \gamma^* e$ with amplitudes as given by (3.1). Their pole structure will differ depending on whether the lepton states are defined by the FSD or the SSD prescription. For the SSD prescription, the mass matrix is by construction diagonal at the scale of m_μ so that the pole at $s = m_\mu^2$ will occur in the amplitude for $\gamma^* \mu \rightarrow \gamma^* \mu$ but not in that for $\gamma^* e \rightarrow \gamma^* e$, which is as it should be. But for the FSD prescription where the mass matrix at the scale m_μ need not be diagonal, both these amplitudes will generally develop a pole at $s = m_\mu^2$. This means that for a process such as $e^+e^- \rightarrow e^+e^-e^+e^-$ as indicated in Figure 3, the cross section will show a sharp resonance peak at $s = m_\mu^2$. The physical meaning of this is clear, namely first a formation of a μ resonance from $\gamma^* e^-$ followed by its decay

into $e^-e^+e^-$. In other words, the apparent FSD anomaly here of the μ pole appearing in the “wrong” channel is the same as that pointed out in [2] of the occurrence of lepton flavour-violating $\mu \rightarrow e^-e^+e^-$ decay. A similar conclusion applies to the pole at $s = m_\tau^2$ occurring in $\gamma^*l_1 \rightarrow \gamma^*l_1$. For SSD, the now 3×3 mass matrix is again by construction diagonal at $s = m_\tau^2$, so that this pole will not appear in any of the four processes $\gamma^*e(\mu) \rightarrow \gamma^*e(\mu)$. But for FSD, this is no longer guaranteed. We conclude, therefore, that with the SSD prescription for defining fermion states, which we ourselves prefer, the amplitude (3.1) has indeed throughout a reasonable s -channel pole structure. But for the FSD case, there is the probable difficulty of lepton poles showing up in wrong channels, unless the prescription is supplemented by conditions making certain rotation matrix elements vanish at the pole positions. One possibility would be to choose to diagonalize the mass matrix at a scale above all the lepton masses and to assume that the mass matrix stops rotating below the scale at which it is diagonalized, which we believe is what is often tacitly assumed in the literature. In what follows, we shall take for granted some such assumption has been made for the FSD case although we are unclear whether this is in fact justified.

Next, we examine the u -channel pole structure. According to (3.1) and (3.4), the amplitude has poles at:

$$u_i = (p_i - k')^2 = m_i^2, \quad (3.7)$$

where we note that, s and t being constrained to be the same for all i ,

$$u_i = 2m_i^2 - s - t \quad (3.8)$$

will generally have different values for different i . Given that in channel i , the minimum value of t in the physical range is:

$$t_{min\ i} = -(s - m_i^2)^2/s, \quad (3.9)$$

the maximum value of u_i in the physical range of the i channel is:

$$u_{i\ max} = m_i^4/s, \quad (3.10)$$

so that for $m_i \neq 0$ the pole in (3.7) lies always outside the physical region as it should. For $m_i = 0$, which is a case we shall frequently encounter when calculating later transmutation in the Dualized Standard Model scheme, the pole lies at $u_i = 0$, right at the edge of the physical range of u_i in the i

channel. However, this value of u_i is not accessible within the physical range of the actual transmutation process for which the minimum value of t is:

$$t_{min} = -(s - m_\alpha^2)(s - m_\beta^2)/s, \quad (3.11)$$

giving, for $m_i = 0$:

$$u_{i \ max} = -m_\alpha^2 - m_\beta^2 + m_\alpha^2 m_\beta^2 / s, \quad (3.12)$$

which is necessarily negative and therefore a finite distance from the pole. We conclude therefore that the amplitude (3.1) will also not be troubled by u -channel poles getting into the physical region whether with the FSD or with the SSD prescription.

We note, of course, that at energy scales different from the actual lepton masses, the poles in the amplitude would have shifted to noncanonical positions by virtue of the running mass eigenvalues. But this would mean only slightly different energy dependences of the cross sections from conventional QED which would not be easily detectable. Nor is this a new phenomenon special to the rotating mass matrix but one common to all theories with running masses, and need not therefore be further scrutinized at present.

Having then passed these tests, the amplitude (3.1) will now be used to calculate cross sections for transmutational processes.

4 Amplitudes with Definite Spins and Polarizations

At the first instance we shall investigate the differential spin- and polarization-summed cross section for the transmutational processes in (1.1). Very elegant invariant methods reducing the spin and polarization sums to traces of γ matrices have of course been developed for calculating these type of cross sections. However, these are not immediately applicable to the amplitude (3.1) here because in taking the absolute value squared of the amplitude there will be crossed terms involving factors such as $u_i(p_i)\bar{u}_j(p_j)$ the summing of which over spin does not give a simple projection operator into positive energy states as in the usual case. Still, of course, the invariant method can be adapted for application to the present rotated amplitude, which indeed has been tried, but this would introduce many more γ matrices and make the calculation of their traces unwieldily complicated.

Mainly for this practical reason, we have chosen to calculate instead the spin- and polarization-summed cross section for (3.1) by the pedestrian method using a specific Lorentz frame and representation of the γ matrices, and then summing the contributions of the various spin and polarization amplitudes. Though less elegant, this has the virtue of being physically more transparent and offers in the future, when conditions are ripe, the means for examining the cross sections for the different spin and polarization components.

We choose to work in the cm frame of one of the channels i for which the kinematics have already been worked out in a previous section, and adopt for γ matrices the Pauli-Dirac representation, namely:

$$\gamma_0 = \begin{pmatrix} 1 & 0 \\ 0 & -1 \end{pmatrix}; \quad \gamma_k = \begin{pmatrix} 0 & \sigma_k \\ -\sigma_k & 0 \end{pmatrix}, \quad (4.1)$$

where σ_k are the standard Pauli matrices. We quantize the spin of all the incoming leptons j along the direction \mathbf{p}_i and of all the outgoing leptons j' along the direction \mathbf{p}'_i , while the photon polarizations we quantize along respectively \mathbf{k} and \mathbf{k}' . This gives for the photon polarization vectors:

$$\epsilon_+(k) = \begin{pmatrix} 0 & 0 & 0 & \sqrt{2} \\ 0 & 0 & 0 & 0 \\ 0 & -\sqrt{2} & 0 & 0 \\ 0 & 0 & 0 & 0 \end{pmatrix}, \quad \epsilon_-(k) = \begin{pmatrix} 0 & 0 & 0 & 0 \\ 0 & 0 & -\sqrt{2} & 0 \\ 0 & 0 & 0 & 0 \\ \sqrt{2} & 0 & 0 & 0 \end{pmatrix}; \quad (4.2)$$

and

$$\begin{aligned} \epsilon_+(k') &= \frac{1}{\sqrt{2}} \begin{pmatrix} 0 & 0 & -i \sin \theta'_i & 1 + \cos \theta'_i \\ 0 & 0 & 1 - \cos \theta'_i & i \sin \theta'_i \\ i \sin \theta'_i & -(1 + \cos \theta'_i) & 0 & 0 \\ -(1 - \cos \theta'_i) & -i \sin \theta'_i & 0 & 0 \end{pmatrix}, \\ \epsilon_-(k') &= \frac{1}{\sqrt{2}} \begin{pmatrix} 0 & 0 & -i \sin \theta'_i & -(1 - \cos \theta'_i) \\ 0 & 0 & -(1 + \cos \theta'_i) & i \sin \theta'_i \\ i \sin \theta'_i & 1 - \cos \theta'_i & 0 & 0 \\ 1 + \cos \theta'_i & -i \sin \theta'_i & 0 & 0 \end{pmatrix}; \end{aligned} \quad (4.3)$$

and for the lepton wave functions with definite spins:

$$u_+(p_j) = \frac{1}{\sqrt{2(E_j + m_j)}} \begin{pmatrix} 0 \\ E_j + m_j \\ 0 \\ \omega_j e^{-i\theta_j} \end{pmatrix},$$

$$u_-(p_j) = \frac{1}{\sqrt{2(E_j + m_j)}} \begin{pmatrix} E_j + m_j \\ 0 \\ -\omega_j e^{-i\theta_j} \\ 0 \end{pmatrix}; \quad (4.4)$$

and:

$$u_+(p'_j) = \frac{1}{2\sqrt{2(E_j + m_j)}} \begin{pmatrix} (E_j + m_j)(1 - e^{-i\theta'_i}) \\ (E_j + m_j)(1 + e^{-i\theta'_i}) \\ \omega_j(e^{i\theta_j} - e^{-i\theta'_j}) \\ \omega_j(e^{i\theta_j} + e^{-i\theta'_j}) \end{pmatrix}, \quad (4.5)$$

$$u_-(p'_j) = \frac{1}{2\sqrt{2(E_j + m_j)}} \begin{pmatrix} (E_j + m_j)(1 + e^{-i\theta'_i}) \\ (E_j + m_j)(1 - e^{-i\theta'_i}) \\ -\omega_j(e^{i\theta_j} + e^{-i\theta'_j}) \\ -\omega_j(e^{i\theta_j} - e^{-i\theta'_j}) \end{pmatrix}. \quad (4.6)$$

In these formulae, we follow the near standard convention, say for example in [13], apart from the removal of a factor $1/\sqrt{m_j}$ in the normalization of $u(p)$ which is more convenient for our case where m_j can be zero.

With the photon polarization vectors in (4.2) and (4.3) and the lepton wave functions in (4.4) and (4.6), it is straightforward to calculate the various spin and polarization amplitudes. We obtain the following, where superscripts denote the photon polarizations and subscripts the lepton spins, while right-hand indices correspond to incoming and left-hand indices outgoing states. By parity, amplitudes are unchanged with the signs of all superscripts and subscripts reversed, and by angular momentum conservation, only two amplitudes are nonzero for the s -channel diagram (a).

$$\begin{aligned} (\mathcal{M}^{(a)})_{++}^{++} &= \frac{-ie^2}{2} \frac{1}{(s - m_j^2)} \{ \omega_i [E_j + m_j + 2\omega_j e^{-i\theta_j} \\ &\quad + (E_j - m_j)e^{-2i\theta_j}] (1 + e^{i\theta'_i}) + 2i\omega_j^2 \sin \theta_j (e^{i\theta'_j} - e^{-i\theta_j}) \}; \\ (\mathcal{M}^{(a)})_{-+}^{-+} &= \frac{-ie^2}{2} \frac{1}{(s - m_j^2)} \{ \omega_i [-E_j - m_j + (E_j - m_j)e^{-2i\theta_j}] (1 - e^{i\theta'_i}) \\ &\quad + 2i\omega_j^2 \sin \theta_j (e^{i\theta'_j} - e^{-i\theta_j}) \}; \\ (\mathcal{M}^{(b)})_{++}^{++} &= \frac{-e^2}{4} \frac{(1 - e^{i\theta'_i})}{(u_j - m_j^2)} \times \\ &\quad \{ 2\omega_j e^{-i\theta_j} [\omega_j \sin \theta_j (1 - \cos \theta'_i) + \omega_i \sin \theta'_i + \omega_j \cos \theta_j \sin \theta'_i] \} \end{aligned}$$

$$\begin{aligned}
& + [(\omega_j^2 - \omega_i E_j + \omega_i m_j) e^{-2i\theta_j} + (\omega_j^2 - \omega_i E_j - \omega_i m_j)] \sin \theta'_i \}; \\
(\mathcal{M}^{(b)})_{-+}^{-+} &= \frac{e^2 (1 + e^{i\theta'_i})}{4 (u_j - m_j^2)} \times \\
& \{ [\omega_j^2 - \omega_i E_j + \omega_i m_j] e^{-2i\theta_j} - [\omega_j^2 - \omega_i E_j - \omega_i m_j] \} \sin \theta'_i \}; \\
(\mathcal{M}^{(b)})_{++}^{-+} &= \frac{e^2 (1 - e^{i\theta'_i})}{4 (u_j - m_j^2)} \times \\
& \{ 2\omega_j e^{-i\theta_j} [\omega_j \sin \theta_j (1 + \cos \theta'_i) + \omega_i \sin \theta'_i - \omega_j \cos \theta_j \sin \theta'_i] \\
& - [(\omega_j^2 - \omega_i E_j + \omega_i m_j) e^{-2i\theta_j} + (\omega_j^2 - \omega_i E_j - \omega_i m_j)] \sin \theta'_i \}; \\
(\mathcal{M}^{(b)})_{-+}^{++} &= \frac{e^2 (1 + e^{i\theta'_i})}{4 (u_j - m_j^2)} \times \\
& \{ [\omega_j^2 - \omega_i E_j + \omega_i m_j] e^{-2i\theta_j} - [\omega_j^2 - \omega_i E_j - \omega_i m_j] \} \sin \theta'_i \}; \\
(\mathcal{M}^{(b)})_{++}^{--} &= \frac{-ie^2 (1 + e^{i\theta'_i})}{4 (u_j - m_j^2)} \times \\
& \{ -2\omega_j e^{-i\theta_j} [(\omega_j \cos \theta_j + \omega_i)(1 + \cos \theta'_i) + \omega_j \sin \theta_j \sin \theta'_i] \\
& + [(\omega_j^2 - \omega_i E_j + \omega_i m_j) e^{-2i\theta_j} + (\omega_j^2 - \omega_i E_j - \omega_i m_j)] (1 + \cos \theta'_i) \}; \\
(\mathcal{M}^{(b)})_{++}^{+-} &= \frac{-ie^2 (1 + e^{i\theta'_i})}{4 (u_j - m_j^2)} \times \\
& \{ 2\omega_j e^{-i\theta_j} [(\omega_j \cos \theta_j - \omega_i)(1 - \cos \theta'_i) - \omega_j \sin \theta_j \sin \theta'_i] \\
& - [(\omega_j^2 - \omega_i E_j + \omega_i m_j) e^{-2i\theta_j} + (\omega_j^2 - \omega_i E_j - \omega_i m_j)] (1 - \cos \theta'_i) \}; \\
(\mathcal{M}^{(b)})_{-+}^{+-} &= \frac{-ie^2 (1 - e^{i\theta'_i})}{4 (u_j - m_j^2)} \times \\
& \{ [\omega_j^2 - \omega_i E_j + \omega_i m_j] e^{-2i\theta_j} - [\omega_j^2 - \omega_i E_j - \omega_i m_j] \} (1 - \cos \theta'_i); \\
(\mathcal{M}^{(b)})_{-+}^{--} &= \frac{-ie^2 (1 - e^{i\theta'_i})}{4 (u_j - m_j^2)} \times \\
& \{ -[\omega_j^2 - \omega_i E_j + \omega_i m_j] e^{-2i\theta_j} + [\omega_j^2 - \omega_i E_j - \omega_i m_j] \} (1 + \cos \theta'_i).
\end{aligned} \tag{4.7}$$

For $j = i$, these amplitudes reduce to the amplitudes for ordinary Compton scattering, affording thus a check of the above expressions.

With these formulae, given the rotation matrix $S_{\alpha i}$, one can then calculate by summing over j the amplitudes (3.1) of any transmutation process $\gamma l_\alpha \longrightarrow \gamma l_\beta$ for any spin and polarization combinations.

5 The Rotation Matrix

Up to the present section, our formalism has been developed generally for any rotating mass matrix, without reference to a particular scheme for how the rotation is generated. However, as can be seen in (3.1), (3.3) and (3.4), the transmutation amplitude depends on the rotation matrix elements $S_{\alpha i}$ and the mass eigenvalues m_i , all of which are functions of the energy scale \sqrt{s} and depend on the scheme or model from which the rotating mass matrix is derived, which has thus now to be specified. In our companion paper [2], two explicit schemes at more or less opposite ends of a spectrum of possibilities were considered, which are also what we have chosen to investigate in detail in this paper. One is the so-called NSM scheme where the rotation of the fermion mass matrix is driven just by the nondiagonal lepton mixing or MNS matrix [4] via the standard renormalization group equations (1.1) and (1.2) in [2] of the (conventional) Standard Model. Lepton states are here defined by the FSD prescription. The other is the so-called DSM (Dualized Standard Model) scheme where the rotation of the mass matrix is driven by new generation-changing forces not normally considered in the Standard Model. In this latter scheme, even the mixing matrices of quarks and leptons are themselves consequences of the mass matrix rotation and even calculable, with the results so far obtained already giving a quite cogent explanation for the characteristic quark and lepton mixing patterns seen in experiment. (See e.g. [12] for a summary.) In this DSM scheme, specification of fermion states by the SSD prescription is essential.

Since these two schemes have already been described in our companion paper [2] with further details given elsewhere in the literature, we shall note here only those points which are of particular relevance to the present calculation. Given that in the NSM scheme, the mass matrix rotation is driven by the nondiagonal mixing matrix, while in the DSM case, the nondiagonal mixing matrix itself results from the mass matrix rotation, it follows that the transmutation effects arising from the rotation will in general be stronger in the DSM than in the NSM scheme. (An exception is the pole effect in “wrong channels” for the NSM scheme, because of the FSD prescription adopted, as already explained in section 3.) And since, as we shall see, transmutation effects are usually quite small, although some can be near the present limit of experimental detectability, it is the DSM scheme which will be examined here in greater detail, being potentially of more immediate experimental interest.

As explained in [2], with its 3 free parameters already fitted to the mass ratios $m_c/m_t, m_\mu/m_\tau$ and the Cabibbo angle [11], the DSM scheme gives a

parameter-free prediction for the rotating mass matrices as a function of the energy scale, which in the case of charged leptons is found in Figure 3 of [2]. As a result, the mass eigenvalues m_i as well as the rotation matrices $S_{\alpha i}$ from the physical states α to the mass eigenstates i are also known at any scale. We have thus all the information needed to carry out the above calculation of transmutation cross sections. Although the accuracy and validity of these predictions are conditioned by the present limitations of the scheme and subject to possible amendments in the future when understanding improves, they will be sufficient for the exploratory purposes of this paper. For ease of reference¹, the values of m_i and $S_{\alpha i}$ are given explicitly in Figure 4.

For the NSM scheme with which we shall do no explicit detailed calculation, we need only note that the mass eigenvalues m_i , like the physical lepton masses, are hierarchical, meaning $m_1 \gg m_2 \gg m_3$, while the rotation matrix $S_{\alpha i}$, like the mass matrix itself, have non-diagonal elements which are zero at the fixed scale chosen for diagonalization and then increase approximately linearly with the logarithm of the energy scale. Their actual values can be calculated from eq. (4.2) of [2].

The mass eigenvalues m_i enter in the diagonal amplitudes \mathcal{M}_i , and the rotation matrix $S_{\alpha i}$ in evaluating the transmutation amplitude with (3.1) where a sum over the eigenstates i has to be performed. In performing this sum, two points of detail are noteworthy. First, in the DSM case, the mass matrix at any scale being a factorizable matrix has always only one non-zero eigenvalue, say m_h which is m_1 for energies above the τ threshold but m_2 below. The amplitudes \mathcal{M}_i above the τ threshold for $i = 2, 3$ are thus identical. Hence, by the unitarity of $S_{\alpha i}$, the sum over i in (3.1) for the transmutation amplitude takes always the following simple form for $\alpha \neq \beta$:

$$\sum_i S_{\alpha i} \mathcal{M}_i S_{\beta i} = S_{\alpha h} S_{\beta h} [\mathcal{M}_h - \mathcal{M}_3]. \quad (5.1)$$

Therefore, if the difference $\mathcal{M}_h - \mathcal{M}_3$ is small compared with the amplitudes themselves, which it often will be, then it is much better to use the latter formula than to do the sum over i directly, for the sum will involve large cancellations, requiring thus knowing $S_{\alpha i}$ to a greater accuracy than is warranted by the DSM scheme in its present form. Also in the NSM scheme,

¹We adopt here the convention of our earlier papers on the DSM in labelling the fermion eigenstates in order of their mass eigenvalues, i.e. with the heaviest labelled as 1, the second as 2, and the lightest as 3, which is more natural in this scheme. Unfortunately, this is the reverse of the the standard convention for labelling neutrinos adopted in [2] which follows the historical order of their discovery.

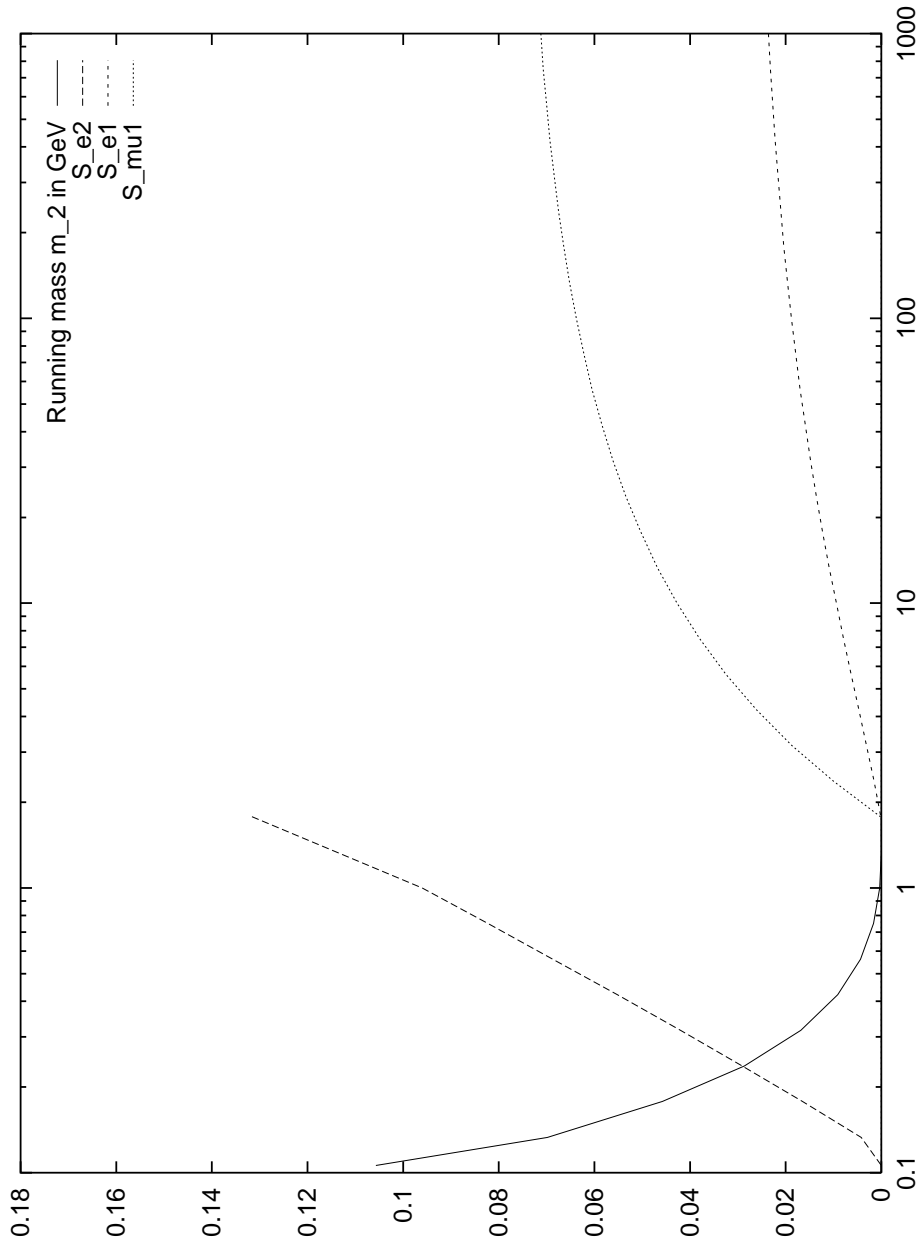


Figure 4: The rotation matrix $S_{\alpha i}$ and the mass eigenvalue m_2 given as functions of the energy scale. By construction, the scheme has $m_1 = m_\tau, m_2 = 0$ at any scale above the τ mass, and $m_3 = 0$ at any scale above the μ mass.

the same statement will apply so long as the fermion mass spectrum is hierarchical for in comparison to the heaviest generation, the two lighter ones will appear degenerate so that the last formula in (5.1) will be a very good approximation.

Secondly, the last formula in (5.1) also offers a link-up of our present calculation to the estimates made in our companion paper [2]. To be specific, consider the s -channel diagram. The amplitudes \mathcal{M}_h and \mathcal{M}_3 differ only in the masses m_h and m_3 where $m_3 \sim 0$. Thus, if m_h is small compared with the energy \sqrt{s} as is often the case, then the difference between the two amplitudes is of order m_h/\sqrt{s} times the amplitude itself. Noting next that $S_{\alpha h}S_{\beta h}m_h = \sum_i S_{\alpha i}S_{\beta i}m_i = \langle \alpha|m|\beta \rangle$, exactly in DSM because $m_i = 0, i \neq h$, and approximately in NSM so long as the spectrum is hierarchical, we conclude that the transmutation amplitude is suppressed compared with that for diagonal processes by a factor $\langle \alpha|m|\beta \rangle/\sqrt{s}$, precisely as suggested in [2].

As we shall see, the formula (5.1) gives also some useful relations between cross sections of different transmutation processes.

6 Spin- and Polarization-Summed Cross Sections

In calculating the cross sections of the various transmutation processes in (1.1), we find it easiest to work in the cm frame of the channel with the lowest lepton mass eigenvalue m_3 , which in the DSM scheme is always zero. Hence in the chosen frame, only the amplitudes for the massive lepton channel h are complicated, while those of the remaining channel(s) reduce just to the cm amplitudes of Compton scattering in the limit $m_e \rightarrow 0$ and take particularly simple forms. Applying then the formula (5.1) to each of the amplitudes in (4.7), summing over all 3 channels above the τ -threshold but over only channels 2 and 3 below the τ -threshold, we obtain the 8 transmutation amplitudes each with a definite combination of polarizations and spins. Taking next the absolute values squared of these amplitudes and summing over all 8 spin and polarization combinations one obtains, for energies measured in GeV, the desired cross section as:

$$\frac{d\sigma}{d\Omega} = \frac{1}{16\pi^2} \frac{\omega'}{\omega} \frac{1}{4s} \sum_{spin} \sum_{pol} |\mathcal{M}|^2 \times 0.3894 \text{ mb/sr.} \quad (6.1)$$

Given that all the variables appearing in (4.7) have already been expressed in terms of the invariants s and t in section 2, we can now evaluate the spin- and polarization-summed cross section as functions of s and t which, we recall, have the same meaning for all the internal channels i as well as for the actual transmutation process $\gamma l_\alpha \rightarrow \gamma l_\beta$.

Following this procedure, we have calculated explicitly the differential cross sections for the following 4 transmutation processes: $\gamma e \rightarrow \gamma \mu(\tau)$ and $\gamma \mu \rightarrow \gamma e(\tau)$, ignoring for the moment τ initiated processes since no τ target or beam is likely to be available in the foreseeable future. Of the 4 processes calculated, the cross sections of $\gamma e \rightarrow \gamma \mu$ and $\gamma \mu \rightarrow \gamma e$ are almost identical for the same values of s and t , as can be easily understood. In all 4 cases, as in ordinary Compton scattering, the cross sections are dominated at most energies by the u -channel pole(s). However, we have found it more convenient to plot the cross sections not as functions of u but as functions of the variable $s+t$ which is close to u but, in contrast to u , has a common meaning for all channels, both internal and external. Above the τ threshold at $\sqrt{s} = 1.777$ GeV all 4 processes occur, the calculated cross sections for which are as presented in the Figures 5, 6, and 7. They are seen to have very similar behaviour. Indeed, the amplitudes for the different processes, according to (5.1), differ at the same values of s and t only by the factors $S_{\alpha 1} S_{\beta 1}$, which depend only on the scale, i.e. \sqrt{s} , but not on t . Hence, apart from small differences due to the kinematical factor in front in (6.1), the plots in Figures 5-7 at the same s are nearly parallel for the different transmutation processes, differing only by the factor $S_{\alpha 1}^2 S_{\beta 1}^2$. In particular, given that the rotation matrix elements shown in Figure 4 are such that $|S_{\tau 1}| > |S_{\mu 1}| > |S_{e 1}|$, it follows that the processes are ordered in size of cross sections as follows: $\gamma \mu \rightarrow \gamma \tau > \gamma e \rightarrow \gamma \tau > \gamma e \rightarrow \gamma \mu$. Notice that, for ease of presentation, it is $d\sigma/d\Omega$ rather than the more usual $d\sigma/du$ that is plotted as a function of $s+t \sim u$ in Figures 5-7. This means that, in spite of appearances, the cross section is actually decreasing rapidly as $s \rightarrow \infty$. Notice further that in all the Figures 5-7, the cross section is given only down to $s+t = 2m_1^2 - m_1^4/s$ for $m_1 = m_\tau$ which is the smallest value of $s+t$ allowed within the physical region for the internal diagonal process $\gamma l_1 \rightarrow \gamma l_1$. Smaller values of $s+t$ than these, down to $s+t = m_\alpha^2 + m_\beta^2 - m_\alpha^2 m_\beta^2/s$ are attained in the actual transmutation process $\gamma l_\alpha \rightarrow \gamma l_\beta$ and for these values of $s+t$, the process $\gamma l_1 \rightarrow \gamma l_1$ can no longer occur so that the transmutation amplitude is now by (5.1) a sum over only the two remaining internal diagonal channels 2 and 3. The plots in the Figures 5-7 of the transmutation cross sections should thus in principle be extended to smaller $s+t$ with values given

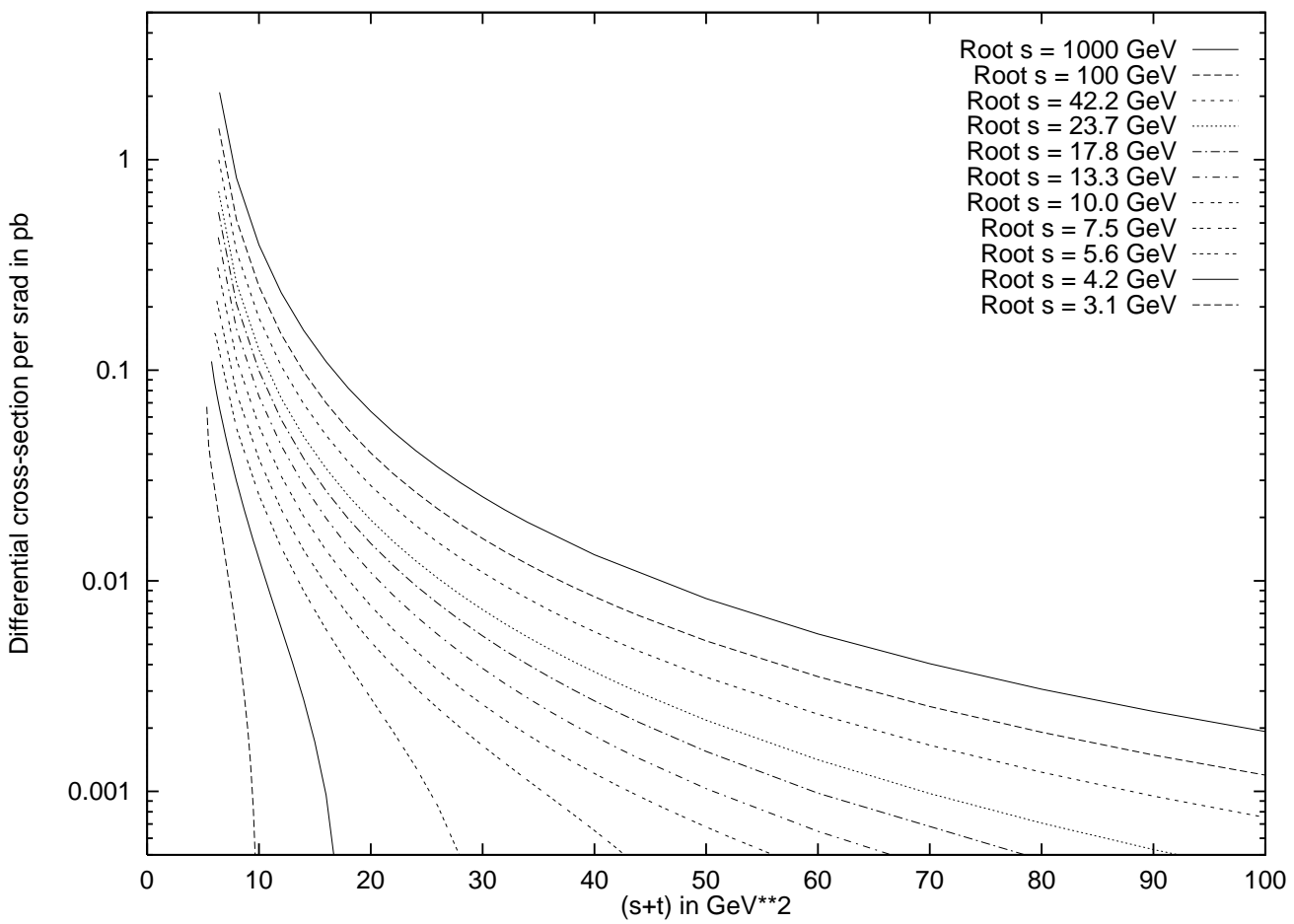


Figure 5: Spin- and polarization-summed differential cross section $d\sigma/d\Omega$ for the transmutation process $\gamma e \rightarrow \gamma \tau$.

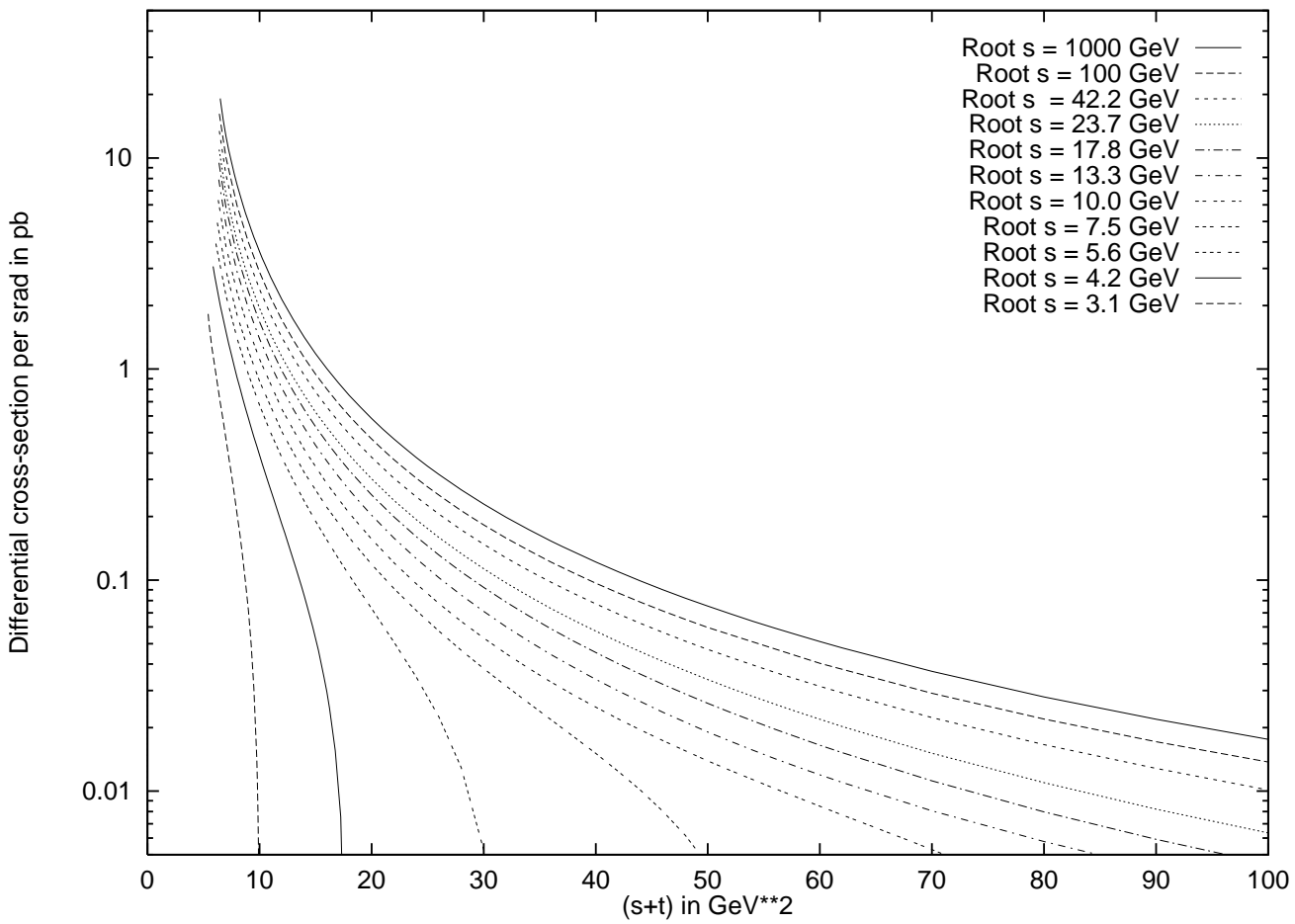


Figure 6: Spin- and polarization-summed differential cross section $d\sigma/d\Omega$ for the transmutation process $\gamma\mu \rightarrow \gamma\tau$.

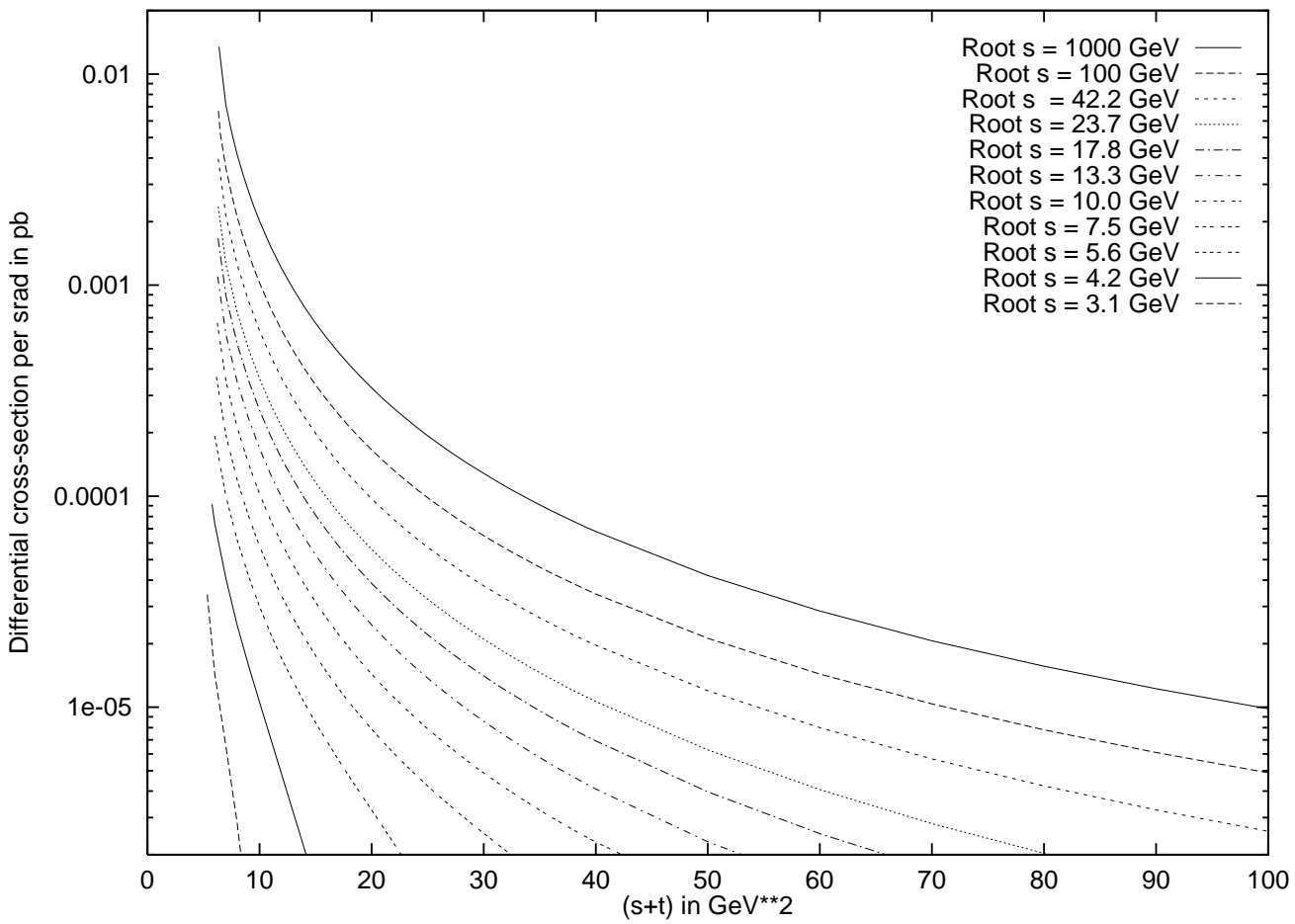


Figure 7: Spin- and polarization-summed differential cross section $d\sigma/d\Omega$ for the transmutation process $\gamma e \rightarrow \gamma \mu$.

by $2S_{\alpha_3}^2 S_{\beta_3}^2$ times the Compton cross section, thus showing a discontinuity at $s + t = 2m_\tau^2 - m_\tau^4/s$. Such extensions are easily calculated but are awkward to present and therefore omitted in our figures. We are in fact uncertain whether the noted discontinuity at $s + t = 2m_\tau^2 - m_\tau^4/s$ will in fact appear in the physical cross section or whether it will be smoothed out by other effects not yet considered.

At energies \sqrt{s} below the τ mass, only the transmutations $\gamma e \rightarrow \gamma \mu$ and $\gamma \mu \rightarrow \gamma e$ can occur with approximately equal cross sections. The result of our calculation for $\gamma e \rightarrow \gamma \mu$ is shown in Figure 8. Though still dominated by the u -channel pole, the cross section has here a more intricate behaviour than at the higher energies shown in Figure 7. First, the mass matrix being by construction in SSD diagonal when the scale equals either the μ or the τ mass, the transmutation cross section is vanishing at both these energies. It thus shows first a rise from zero at the threshold $\sqrt{s} = m_\mu$ of the reaction to a maximum shortly above, and then falls to zero again at $\sqrt{s} = m_\tau$. Secondly, although the mass matrix here has again just one nonzero eigenvalue as for \sqrt{s} above the τ mass, this nonzero eigenvalue m_2 itself approaches zero as $\sqrt{s} \rightarrow m_\tau$. In fact, as can be seen in Figure 4, m_2 remains rather small all the way until \sqrt{s} approaches m_μ , where of course it equals m_μ by construction. Hence, in contrast to the high s situation in Figure 5-7, the smallest value of $s + t$, namely $2m_2^2 - m_2^4/s$, within the physical region of the internal process $\gamma l_2 \rightarrow \gamma l_2$, is in this case usually smaller than the smallest value of $s + t$, namely $m_e^2 + m_\mu^2 - m_e^2 m_\mu^2/s$, within the physical region of the actual transmutation process $\gamma e \rightarrow \gamma \mu$ under consideration. For this reason, in Figure 8, the cross section is given down to $s + t = m_e^2 + m_\mu^2 - m_e^2 m_\mu^2/s$ without showing any discontinuity in $s + t$, although, in principle, at energies where this limit can become smaller than $s + t = 2m_2^2 - m_2^4/s$, similar remarks to those given at the end of the last paragraph also apply. By numerically integrating the differential cross section given in Figure 8, one obtains approximately the total cross section for the process $\gamma e \rightarrow \gamma \mu$ shown in Figure 9, which shows an intriguing maximum at cm energy of about 180 MeV.

Although the above calculation has been performed in detail only for the DSM scheme, from this the transmutation cross sections for the NSM, or indeed any other rotation, scheme can also readily be inferred. In general, of course, the mass matrix has no reason to have two zero eigenvalues as in the DSM case, but the mass eigenvalues must still be hierarchical, meaning that $m_1 \gg m_2 \gg m_3$. In such a case, given that $m_2 - m_3$ is necessarily much smaller than $m_1 - m_2$ or $m_1 - m_3$, we can neglect in the amplitudes

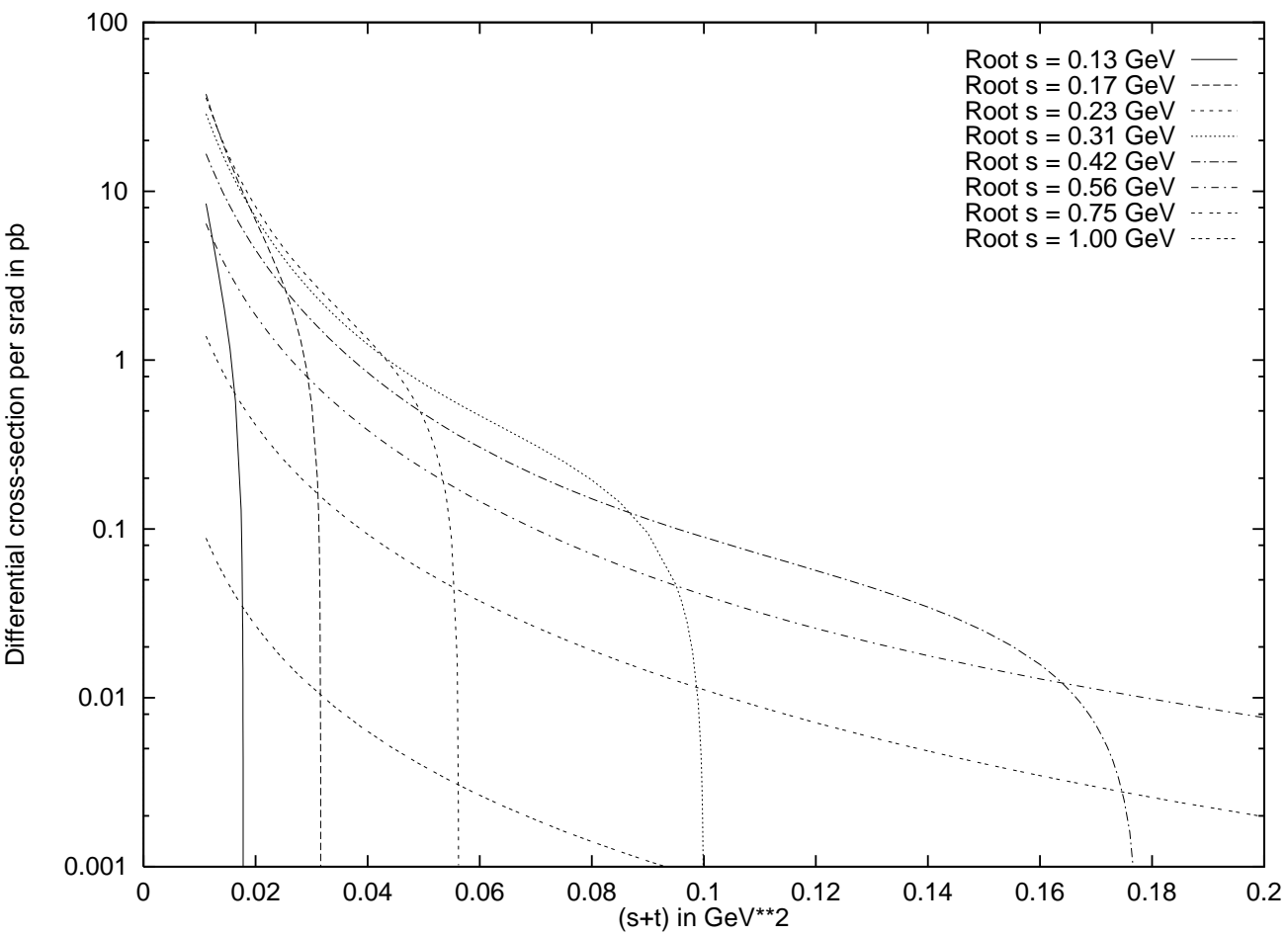


Figure 8: Spin- and polarization-summed differential cross section $d\sigma/d\Omega$ for the transmutation process $\gamma e \rightarrow \gamma \mu$ below τ threshold.

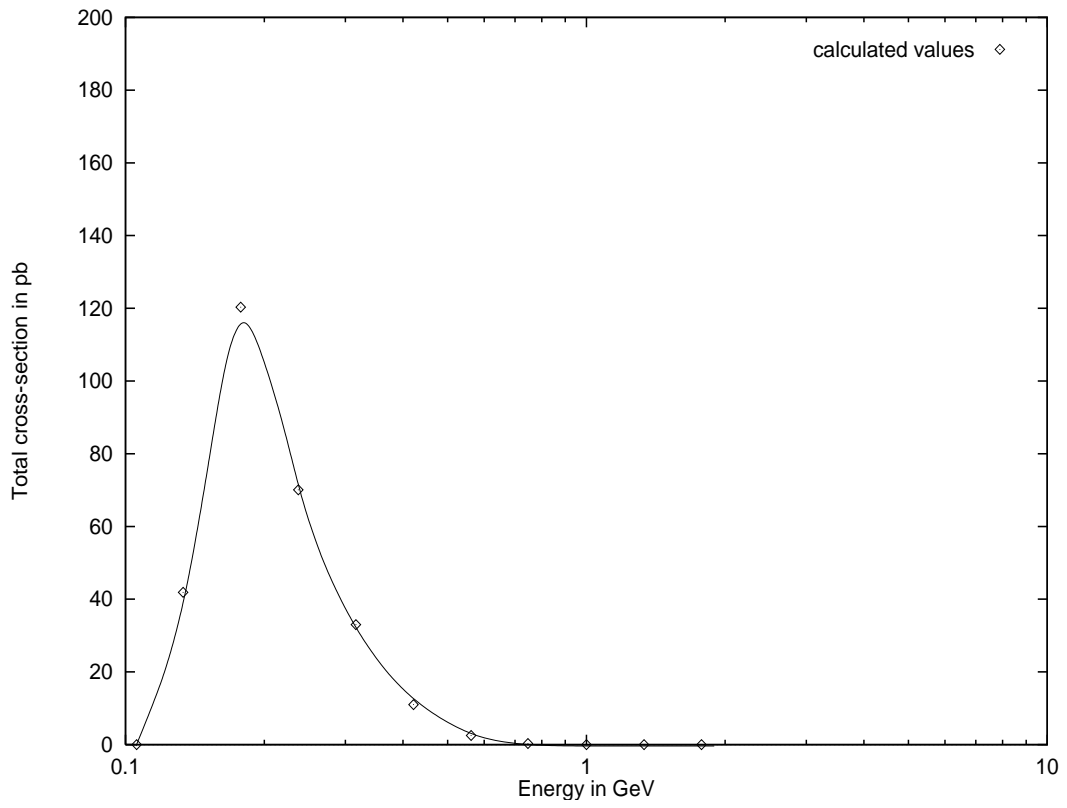


Figure 9: Total cross section for the transmutation process $\gamma e \rightarrow \gamma \mu$ below the τ threshold.

the difference $\mathcal{M}_2 - \mathcal{M}_3$ compared with the difference $\mathcal{M}_1 - \mathcal{M}_3$ so that the expression in (5.1) remains approximately valid. Then at energies above the τ mass, the mass m_1 being necessarily close to m_τ , the cross section will be approximately given just by re-scaling the cross section for DSM at the same value of $s + t$ by a factor $[S_{\alpha 1}^2 S_{\beta 1}^2]_{any} / [S_{\alpha 1}^2 S_{\beta 1}^2]_{DSM}$. For example, for the transmutation $\gamma\mu \rightarrow \gamma\tau$ in NSM from equation (4.2) of [2] one obtains $S_{\mu 1} S_{\tau 1} \sim \langle \mu | m | \tau \rangle / m_1$. At $\sqrt{s} = 17.8$ GeV, say, one decade above the τ mass when the mass matrix is diagonal, $S_{\mu 1} S_{\tau 1} \sim 3 \times 10^{-3}$ compared with $\sim 5 \times 10^{-2}$ for DSM as read from Figure 4 here. Hence the differential cross section at this energy for NSM is just given by multiplying the curve at the same energy in Figure 6 of this paper by a factor $\sim (0.06)^2$, i.e. some 2–3 orders smaller. At scales below the τ mass, this simple criterion no longer works, but here in any case the NSM scheme has presumably to be modified in view of the apparent difficulty with the “pole in the wrong channel” mentioned above, so that one is yet in no position to calculate the transmutation cross section.

7 Remarks

Our first aim in this paper is to examine the possibility of, and if possible to develop the methodology for, calculating cross sections of transmutation processes when the fermion mass matrix rotates with changing scales, using photo-transmutation as a specific example. One ends up with a procedure which seems both to be internally consistent and to give reasonable answers, while offering a chance for generalization to other processes. The procedure was constructed following a certain line of logic, although one cannot pretend in any sense to have derived it from first principles. One can thus hope that it will serve at least as a working hypothesis for exploring the unfamiliar physics involved. Even with the method so developed, the calculation still depends on the physics mechanism driving the rotation of the mass matrix, and the result one obtains, of course, can at best be as good as the physics mechanism from which it is deduced. We have investigated two particular schemes labelled respectively as NSM and DSM. Although we are biased towards the second, this being the scheme we ourselves suggested and advocate, we are aware of some shortcomings [14] and its need for further refinement. The results in either scheme therefore have yet to be taken with caution.

With these reservations in mind, let us proceed to analyse the results obtained. We have not as yet made a thorough study as regards their ac-

cessibility to tests by experiment. Some general observations, however, are already possible. In looking for photo-transmutation effects, one need not restrict oneself to real photons but can make free use of the virtual photons available in e^+e^- colliders.² However, the cross sections at energies above the τ mass being in general rather small, namely at most in the low picobarn or multi-femtobarn range shortly above the τ threshold, and decreasing rapidly with increasing energy, it seems unlikely that they would have been observed without a conscious search for them. This is true for both the NSM and DSM schemes. To ascertain whether some of the effects would be observable in existing machines such as LEP or BEPC, some closer study would be necessary, which is underway. The cross section being much larger for transmutation of e into τ than of e into μ , as can be seen in Figures 5 and 7 for DSM, a search for τ seems indicated. In the future, when μ storage rings become available then a search for the transmutation for μ into τ looks even better because of the larger cross section, as seen in Figure 6 for DSM. The same remarks should hold also for NSM.

To look for e to μ transmutation, it would be much more profitable to work at low energy below the τ threshold at cm energy of around 200 MeV, where the cross section in DSM has a maximum, as can be seen in Figure 9. At first sight, the predicted cross section being of the order of 100 picobarns, it seems surprising that the effect have not been seen already by experiment, but we have not yet succeeded in locating any relevant data on γe collisions in that energy region. The reason seems to be that with electrons having a mass of only half an MeV, it will take 40 GeV photons impinging on a stationary electron target to make up a cm energy of 200 MeV, and real photon beams of such an energy are not readily available. One can hope to make up the desired energy also by shining laser light on to one of the two beams in an electron-positron collider, or else the back-scattered light from one beam on to the other, but none of the existing colliders we looked at seem to have just the right beam energies for this purpose, although it would not be difficult of course to achieve this energy for a purpose-built collider. Otherwise, one can utilize again the virtual photons available in e^+e^- colliders, in which case low energy colliders like BEPC would seem to be more appropriate.

As far as searching for transmutational effects is concerned, there is no reason of course to restrict to photo-transmutations. The same general considerations can be applied to other processes, e.g. to e^+e^- collision itself

²We are grateful to John Guy for a reminder and subsequent discussion for this possibility.

giving transmutations like $e^+e^- \rightarrow e^+\mu^-$. The cross sections for these processes have not yet been calculated but from the experience gained in this paper, one can hope that the methodology developed here can be adapted to e^+e^- collision with only moderate modifications. If so, then our result in Figure 9 for photo-transmutation suggests that there may also be a maximum in the cross section for $e^+e^- \rightarrow e^+\mu^-$ at cm energy of a few hundred MeV.

In any case, there can be a wide field here for future experimental investigation.

References

- [1] See e.g. B. Grzadkowski, M. Lindner and S. Theisen, Phys. Lett. B198, 64, (1987); H. Arason, D.J. Castaño, B. Kesthelyi, S. Mikaelian, E.J. Piard, P. Ramond and B.D. Wright, Phys. Rev. D46 (1992) 3945.
- [2] José Bordes, Chan Hong-Mo and Tsou Sheung Tsun, hep-ph/0006338.
- [3] N. Cabibbo, Phys. Rev. Lett. 10, 531 (1963); M. Kobayashi and T. Maskawa, Prog. Theor. Phys. 49, 652 (1973).
- [4] Z. Maki, M. Nakagawa and S. Sakata, Prog. Theor. Phys. 28 (1962) 247.
- [5] T. Kafka, Nucl. Phys. B (Proc. Suppl.) 35, 427, (1994); M. Goodman, *ibid* 38, 337, (1995); W.W.M. Allison et al., Phys. Letters B391, 491, (1997).
- [6] CHOOZ collaboration, M. Apollonio et al., Phys. Lett. B420, 397, (1997).
- [7] Y. Fukuda et al, Super-Kamiokande Collaboration, Phys. Lett. B433 (1998) 9; Phys. Lett. B436 (1998) 33; Phys. Rev. Lett. 81 (1998) 1562.
- [8] Chan Hong-Mo and Tsou Sheung Tsun, Phys. Rev. 57D, (1998) 2507, hep-th/9701120.
- [9] José Bordes, Chan Hong-Mo, Jacqueline Faridani, Jakov Pfauder, and Tsou Sheung Tsun, Phys. Rev. D58, 013004, (1998), hep-ph/9712276.
- [10] José Bordes, Chan Hong-Mo, Jakov Pfauder and Tsou Sheung Tsun, Phys. Rev. D58 (1998) 053003, hep-ph/9802420; Phys. Rev. D58 (1998) 053006, hep-ph/9802436.

- [11] José Bordes, Chan Hong-Mo and Tsou Sheung Tsun, hep-ph/9901440, Eur. Phys. J. C10 (1999) 63.
- [12] Chan Hong-Mo, to appear in the proceedings of *Intern. Conf. on Fundamental Sciences: Mathematics and Theoretical Physics*, March 2000, Singapore.
- [13] F. Mandl and G. Shaw, *Quantum Field Theory*, John Wiley and Sons, 1984.
- [14] Chan Hong-Mo and Tsou Sheung Tsun, Int. J. Mod. Phys. A14 (1999) 2173, hep-ph/9904406.